International Journal of Pharmaceutics 418 (2011) 42–53

Contents lists available at ScienceDirect

International Journal of Pharmaceutics

journal homepage: www.elsevier.com/locate/ijpharm

Mathematical modeling of drug release from lipid dosage forms

J. Siepmann[a,b,*], F. Siepmann[a,b]

[a] Univ. Lille Nord de France, College of Pharmacy, 3 Rue du Prof. Laguesse, 59006 Lille, France
[b] INSERM U 1008, Controlled Drug Delivery Systems and Biomaterials, 3 Rue du Prof. Laguesse, 59006 Lille, France

ARTICLE INFO

Article history:
Received 10 June 2011
Received in revised form 11 July 2011
Accepted 13 July 2011
Available online 23 July 2011

Keywords:
Mathematical modeling
Lipid
Drug release mechanism
Controlled release
Implant
Microparticle

ABSTRACT

Lipid dosage forms provide an interesting potential for controlled drug delivery. In contrast to frequently used poly(ester) based devices for parenteral administration, they do not lead to acidification upon degradation and potential drug inactivation, especially in the case of protein drugs and other acid-labile active agents. The aim of this article is to give an overview on the current state of the art of mathematical modeling of drug release from this type of advanced drug delivery systems. Empirical and semi-empirical models are described as well as mechanistic theories, considering diffusional mass transport, potentially limited drug solubility and the leaching of other, water-soluble excipients into the surrounding bulk fluid. Various practical examples are given, including lipid microparticles, beads and implants, which can successfully be used to control the release of an incorporated drug during periods ranging from a few hours up to several years. The great benefit of mechanistic mathematical theories is the possibility to quantitatively predict the effects of different formulation parameters and device dimensions on the resulting drug release kinetics. Thus, *in silico* simulations can significantly speed up product optimization. This is particularly useful if long release periods (e.g., several months) are targeted, since experimental trial-and-error studies are highly time-consuming in these cases. In the future it would be highly desirable to combine mechanistic theories with the quantitative description of the drug fate *in vivo*, ideally including the pharmacodynamic efficacy of the treatments.

1. Introduction

Lipid dosage forms provide a great potential for: (i) the time-controlled release of drugs (Opdebeeck and Tucker, 1993; Kreye et al., 2008; Schulze and Winter, 2009), and (ii) increasing the apparent solubility of poorly water-soluble drugs. This review addresses the first types of dosage forms. The idea is to embed one or more drugs within a lipid matrix, which prevents immediate release (Kaewvichit and Tucker, 1994). In contrast to frequently used poly(ester) [e.g. poly(lactic-co-glycolic acid) (PLGA)] based devices, the creation of acidic environments within the dosage forms upon matrix former degradation can be avoided. For this reason, lipid controlled drug delivery systems are particularly interesting for protein drugs and other acid-labile active agents (Wang, 1989; Khan et al., 1991; Mohl and Winter, 2004; Koennings et al., 2006). The fact that drug release is time-controlled can help overcoming frequent administration (e.g., daily injections), required in the case of active agents with short half-lives, which are rapidly eliminated from the living body.

So far, especially *lipid* microparticles, spherical beads and cylindrical implants have been described for controlled drug delivery. Various preparation methods have been proposed (e.g., compression, extrusion, melting & casting techniques, emulsification methods) and the obtained systems have been characterized: mainly *in vitro*, whereas only a relatively limited number of *in vivo* studies has been reported (e.g., Khan et al., 1993). A broad range of lipids, lipid blends and the addition of other excipients, such as water-soluble "pore formers" has been suggested (Herrmann et al., 2007a). Often, the optimization of this type of advanced drug delivery systems is cumbersome, since relatively long release periods (e.g., several months) are targeted, rendering series of trial-and-error experiments particularly time-consuming. Thus, there is an obvious need for reliable *in silico* optimization tools. Mathematical modeling of the physico-chemical processes involved in the control of drug release can potentially allow for significantly accelerated product development (Siepmann and Peppas, 2001; Siepmann and Goepferich, 2001; Siepmann et al., 2006). This is the case for *mechanistic* mathematical theories, which quantitatively take into account mass transfer processes, such as water and drug diffusion, drug dissolution, and potentially the leaching of other excipients into the surrounding bulk fluid (Crank, 1975; Guse et al., 2006a; Siepmann and Siepmann, 2008). Nevertheless, caution must be paid and the potential violation of assumptions such theories are built on must be considered on a case-by-case basis. In addition,

* Corresponding author at: Univ. Lille Nord de France, College of Pharmacy, INSERM U 1008, 3 Rue du Professeur Laguesse, 59006 Lille, France.
Tel.: +33 3 20964708; fax: +33 3 20964942.
E-mail address: juergen.siepmann@univ-lille2.fr (J. Siepmann).

0378-5173/$ – see front matter © 2011 Elsevier B.V. All rights reserved.
doi:10.1016/j.ijpharm.2011.07.015

mechanistic mathematical theories allow for a better understanding of the underlying drug release mechanisms in a particular type of dosage forms (Fan and Singh, 1989; Vergnaud, 1993). For example, the potential importance of limited drug solubility or structural changes within the system during drug release can be elucidated.

It has to be pointed out that there is no overall, general mathematical theory, which is valid for all types of lipid dosage forms. The type of lipid(s), drug(s), potentially other excipients, relative composition of the system and manufacturing procedure might significantly affect the importance of the physico-chemical processes involved in the control of drug release. Ideally, an appropriate, mechanistic theory is identified/developed based on comprehensive sets of experimental results (Siepmann and Siepmann, 2008). Also, the validity of a particular theory for a specific type of systems should be confirmed by comparison of theoretical *predictions* (e.g., of the impact of device dimensions on the resulting drug release rate) with *independent* experimental results, obtained only after the predictions were made. *Fitting* a model to experimental results (and, thus, optimizing one or more parameters in order to minimize differences between theory and experiment) and obtaining good agreement between theory and experiment is not a real proof for the validity of a model (especially if several parameters are optimized simultaneously). Several mechanistic theories quantifying drug release from lipid dosage forms are described in this review.

In contrast, *empirical* and *semi-empirical* mathematical models often only allow for a quantitative description of drug release, but not for the prediction of the impact of formulation parameters/device dimensions, nor for the elucidation of the underlying drug release mechanisms. Thus, their field of application is much narrower. Great care must be taken, when drawing mechanistic conclusions based on fittings of semi-empirical models to sets of experimentally measured drug release kinetics.

The "father" of mathematical modeling of drug release is Takeru Higuchi, who published his famous square root of time equation in 1961 (Higuchi, 1961). It is a surprisingly simple equation, being mechanistically realistic for a rather complex type of drug delivery systems and illustrates how useful and easy the use of mathematical modeling can be. This review article is part of the special issue of the International Journal of Pharmaceutics, which is dedicated to the 50th anniversary of the classical Higuchi equation.

2. Physico-chemical characterization

In order to be able to mathematical model drug release from a lipid pharmaceutical dosage form, the latter should first be characterized physico-chemically as thoroughly as possible, before and upon exposure to appropriate release media. Highly useful measurements include for example:

(i) Drug release studies under conditions, which best simulate the expected *in vivo* environment;
(ii) Water uptake studies, e.g. gravimetrically (Kreye et al., 2011);
(iii) Dry mass loss studies, e.g. gravimetrically (Kreye et al., 2011);
(iv) Monitoring of dimension changes, e.g. macro- or microscopically (Kreye et al., 2011a);
(v) Morphological studies, e.g. using scanning electron microscopy (SEM) (Koennings et al., 2007a; Schwab et al., 2009);
(vi) Porosity measurements, e.g. using a helium pycnometer (Siepmann et al., 2008);
(vii) Monitoring of drug and water distribution within the implants and time-dependent changes thereof, e.g. using confocal microscopy (Koennings et al., 2007b,c);
(viii) Measurement of thermal system properties, e.g. using Differential Scanning Calorimetry (DSC) (Windbergs et al., 2009);
(ix) X-ray diffraction (Windbergs et al., 2009);
(x) Wettability measurements, e.g. via contact angle determinations (Koennings et al., 2007a);
(xi) Measurement of mechanical properties, e.g. using a texture analyzer (Kreye et al., 2011b).

The obtained information is decisive for the appropriate choice of the mathematical model for a specific type of drug delivery system. For example, if the outer dimensions of the device remain constant during drug release (no significant swelling or erosion), "stationary boundary conditions" can generally be considered, rending a mechanistically realistic mathematical treatment much simpler compared to the case of "moving boundary conditions". The latter might for instance be caused by the presence of a significantly swelling excipient within the system, such as distearoyl-phosphatidyl-choline (Guse et al., 2006b).

Thermal analysis and X-ray diffraction can help to identify the physical state of the lipid(s), drug(s) and potentially other excipients within the systems (Kreye et al., 2011). This can be particularly decisive in the case of compounds, which can crystallize in different forms, exhibiting different key properties, such as solubility in aqueous solutions. Furthermore, the impact of the environmental conditions on drug release should be studied. For instance, Schwab et al. (2009) investigated the effects of the presence of lipases in the release medium *in vitro* on the degradation of lipid dosage forms: microparticles were shown to degrade much faster than macroscopic implants under these conditions.

Fig. 1 shows an example for very interesting experimental results, which can significantly help to identify/develop the appropriate type of mathematical theory for a particular type of drug delivery system. Confocal microscopy was used to localize the model protein "bovine serum albumin" (BSA) [labeled with fluorescein isothiocyanate (FITC)] in glyceryl trimyristate based implants (prepared by compression) before and after exposure to the release medium. In addition, sulforhodamine 101 hydrate (SRH) was dissolved in the bulk fluid (phosphate buffer pH 7.4 in this example). The spatial distribution of the two compounds (FITC-BSA and SRH) was monitored as a function of time in radial and axial cross-sections of the implants (Koennings et al., 2007b). The yellow color in Fig. 1 indicates the presence of the labeled protein, the red color the presence of SRH (and, thus, of water). Protein and "water" concentration profiles (assuming that water penetrates at the same rate as SRH) could be calculated from these images, examples are plotted in the left column in Fig. 1 (black curves indicate labeled protein, gray curves "water"). Very clearly, the release of the protein out of the implants and "water" penetration into the systems are intimately related: upon exposure to the release medium the buffer first penetrates into the surface-near regions of the implants and the protein is released from these areas. Importantly, "water" penetration into the lipid implants takes time in this example: even after 9 d exposure to the aqueous bulk fluid, the core of the formulation is still not fully "wetted" (under the condition that the penetration of the SRH is as fast as water penetration). Interestingly, "water" penetration seems to be more rapid in radial direction than in axial direction within these implants: the thickness of the red "zones" in radial direction is larger than the thickness of the red "zones" in axial direction after 6 and 9 d, as it can be seen in the right column in Fig. 1. This anisotropic behavior can probably be explained by the layered structure of these implants: Fig. 2 shows a confocal microscopy picture of an axial cross-section of an implant after complete protein release and complete SRH penetration into the system. The marked black areas are preferentially oriented in horizontal direction. This might be due to the manufacturing process of these

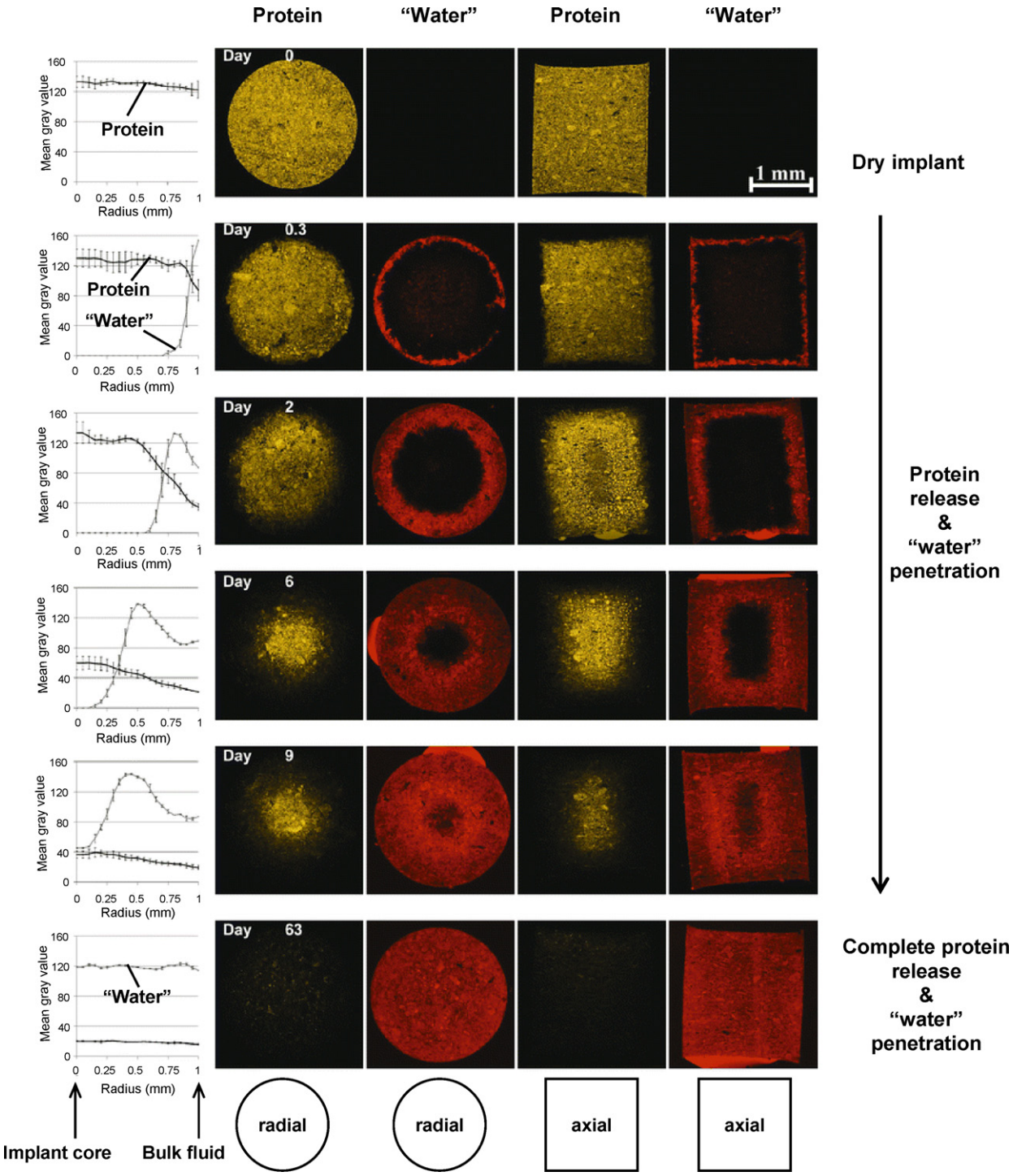

Fig. 1. Monitoring of protein and "water" distribution in glyceryl trimyristate based implants upon exposure to phosphate buffer pH 7.4 using confocal microscopy: the yellow color indicates the labeled protein "fluorescein isothiocyanate-bovine serum albumin" (FITC-BSA). The red color indicates sulforhodamine 101 hydrate (SRH), being dissolved in the bulk fluid surrounding the implants. The left column shows radial distributions of the labeled BSA and SRH within the systems at the indicated time points (obtained from image analysis; black curves = FITC-BSA, gray curves = SRH). The subsequent two columns show radial cross-sections of the implants, the two columns on the right hand side axial cross-sections of the systems. (For interpretation of the references to color in this figure legend, the reader is referred to the web version of the article.) Adapted from Koennings et al. (2007b).

implants: they were prepared by compression. During the compression step the force is applied in axial, and not in radial direction, resulting in a potential preferential orientation of the lipid particles in horizontal direction. It has to be pointed out that so far there is a lack of mathematical theories taking this fact adequately into account.

An interesting study on the impact of the presence of a surfactant in the release medium on lysozyme release from lipid implants has been reported by Koennings et al. (2007a). Fig. 3 shows the experimentally measured protein release kinetics in phosphate buffer pH 7.4 free of Tween 20 (Fig. 3A) versus phosphate buffer pH 7.4 containing 0.1% Tween 20 (Fig. 3B). Very clearly, lysozyme release

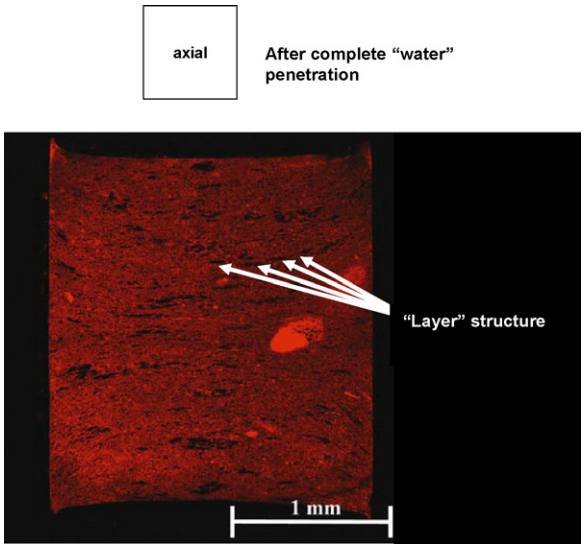

Fig. 2. Confocal microscopy picture of an axial cross-section of a glyceryl trimyristate based implant after 100% protein release and complete phosphate buffer penetration into the system. The red color indicates SRH, which was dissolved in the release medium. (For interpretation of the references to color in this figure legend, the reader is referred to the web version of the article.)
Adapted from Koennings et al. (2007b).

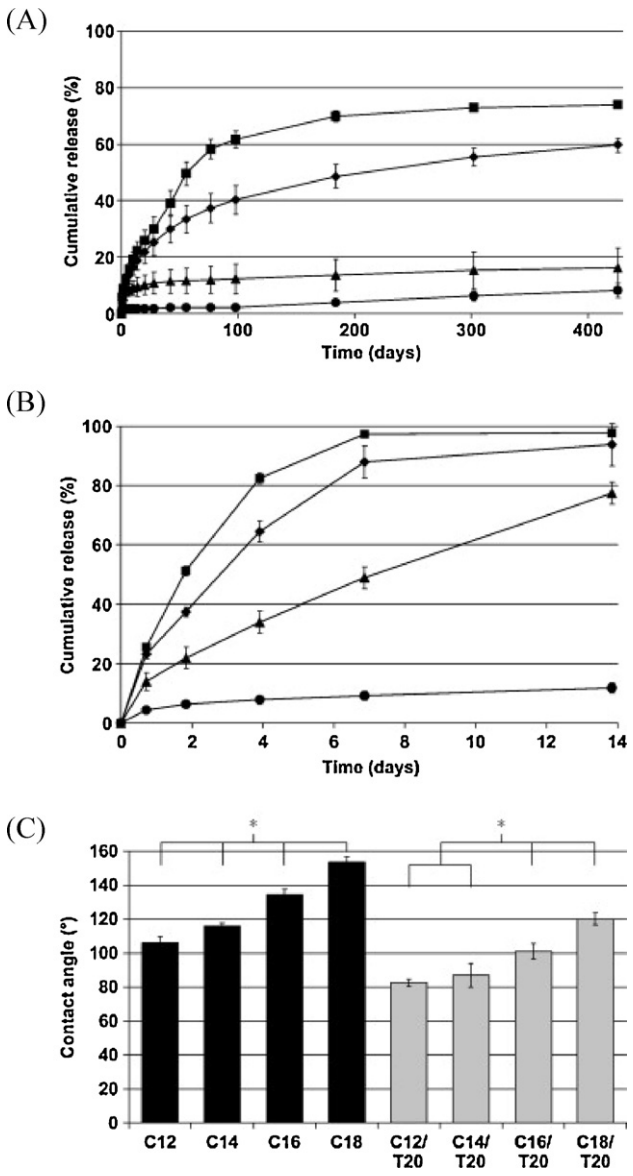

Fig. 3. Impact of the type of lipid on: (A) lysozyme release from lipid implants in phosphate buffer pH 7.4 (squares = glyceryl trilaurate; diamonds = glyceryl trimyristate; triangles = glyceryl tripalmitate; circles = glyceryl tristearate); (B) lysozyme release from lipid implants in phosphate buffer pH 7.4 containing 0.1% Tween 20 (same symbols; note the different scaling of the *x*-axes); and (C) the contact angle of phosphate buffer pH 7.4 (black bars) and buffer containing 0.1% Tween 20 (T 20, gray bars) (C12 = glyceryl trilaurate; C14 = glyceryl trimyristate; C16 = glyceryl tripalmitate; C18 = glyceryl tristearate) (the asterisks indicates $p < 0.01$ in statistical evaluation).
Reprinted with permission from Koennings et al. (2007a).

was much faster in the presence of the surfactant in the bulk fluid (note the different scaling of the *x*-axes). This was true, irrespective of the type of studied lipid matrix former (indicated in the diagrams). The reason for this tremendous impact is probably facilitated wetting and water penetration into the lipid implants in the presence of the surfactant: Fig. 3C shows the experimentally measured contact angle of phosphate buffer pH 7.4 only (black bars) and buffer containing 0.1% Tween 20 (T 20, gray bars) on spin-cast lipid films. As it can be seen, the presence of the surfactant significantly reduces the contact angle in all cases (gray versus black bars). These results can serve as an indication that water penetration into the lipid system might play a major role for the control of drug release.

It has to be pointed out that up to date, the large majority of the characterization studies of lipid dosage forms have been conducted *in vitro*. Only a limited number of reports have been published describing the fate of this type of advanced drug delivery systems and their biocompatibility *in vivo* (Koennings et al., 2007c). For example, Guse et al. (2006b) studied glyceryl tripalmitate based implants prepared by compression containing different amounts of cholesterol or distearoyl-phosphatidyl-choline (DSPC) upon s.c. implantation in mice. They demonstrated good biocompatibility of glyceryl tripalmitate and cholesterol and increased inflammatory reactions with increasing DSPC contents. During 60 d no noteworthy erosion was observed with glyceryl tripalmitate based implants (optionally containing cholesterol). In contrast, the addition of DSPC led to clearly visible signs of degradation and implant swelling. Koennings et al. (2007c) demonstrated biocompatibility of glyceryl tripalmitate based implants comparable to silicone reference cylinders upon administration in the striatum of rat brains. Furthermore, Schwab et al. (2008) measured the resulting serum concentrations of IFN-α in rabbits upon s.c. administration of glyceryl tristearate based implants. The *in vivo* efficacy of lipid controlled release dosage forms was for instance demonstrated by Wang (1989). He administered insulin-loaded, stearic acid-based implants (prepared by compression) subcutaneously into Wistar rats suffering from streptozotocin-induced diabetes. Importantly, the resulting blood glucose levels were highly promising. Khan et al. (1993) prepared bovine serum albumin (BSA)-loaded lipid implants, also via compression. BSA served as model antigen in this case, cholesterol and/or hydrogenated egg lecithin as lipid matrix formers. The systems were subcutaneously administered into mice and the latter's BSA antibody response was monitored. Interestingly, the sustained release of BSA from the implants induced anti-BSA antibodies at 2 months and maintained the same levels of antibodies for up to 10 months. Importantly, this response was more pronounced than that induced by three injections of the same BSA dose (studied for reasons of comparison). However, due to the limited amount of experimental results obtained with lipid dosage forms obtained *in vivo* (and the complexity of the involved phenomena), there is still a significant lack of appropriate mathematical

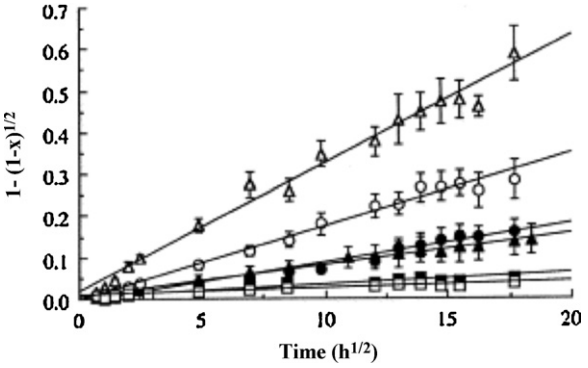

Fig. 4. Plot of "$1-(1-x)^{0.5}$" versus square root of time for *in vitro* release of interferon-α (IFN-α) release from lipid cylindrical matrices based on tetraglycerol tripalmitate (squares), tetraglycerol monopalmitate (filled triangles), tetraglycerol dipalmitate (filled circles), tetraglyerol distearate (open circles), or tetraglyerol monostearate (open triangles).
Reprinted with permission from Yamagata et al. (2000).

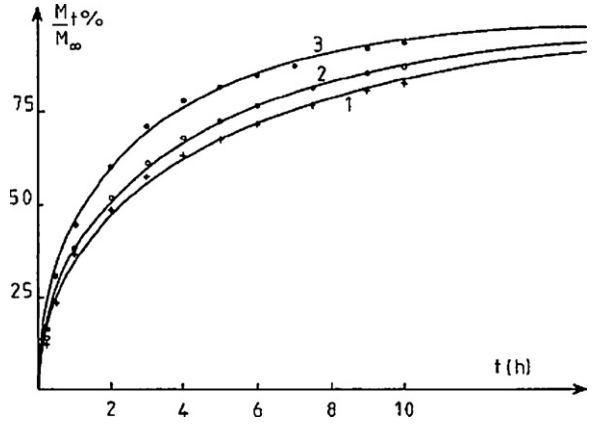

Fig. 5. Sodium salicylate release (M_t and M_∞ represent the cumulative absolute amounts of drug released at time t and infinity) from Gelucire 46/07 based spherical beads in simulated gastric fluid: experiment – symbols and theory – Eq. (2). The "1" indicates 264 mg beads with a radius of 0.36 cm exposed to 200 mL release medium, the "2" beads of 187 mg with a radius of 0.33 cm exposed to 200 mL release medium and the "3" indicates beads of 92 mg with a radius of 0.268 cm exposed to 100 mL release medium.
Reprinted with permission from Bidah et al. (1992).

models quantifying drug release from this type of advanced drug delivery systems in living organisms.

3. Empirical and semi-empirical mathematical models

Empirical and semi-empirical mathematical models can be used to describe experimentally observed drug release, but great caution must be paid when drawing conclusions on the underlying mass transport mechanisms or when making predictions. A frequently applied semi-empirical model is the so-called "power law", or "Peppas-equation", since it was first introduced by Nicholas Peppas in the field of pharmaceutics (Peppas, 1985). Examples for the application of this model are given by Soo et al. (2008), studying the release of paclitaxel from chitosan-phosphatidylcholine based implants, and by Oezyazici et al. (2006), investigating metronidazole release from different types of lipid matrix tablets. Also first order, the Higuchi or Hixson–Crowell equations might be fitted to experimentally determined drug release kinetics (e.g., Karasulu et al., 2003; Allababidi and Shah, 1998). Fig. 4 shows examples for fittings of the following semi-empirical equation to sets of IFN-α release kinetics from different types of lipid matrices:

$$1-(1-x)^{0.5} = kt^{0.5} \quad (1)$$

where x is the fraction of protein released at time t, and k is a constant. The symbols in Fig. 4 represent the experimentally measured drug release kinetics, the straight lines the fitted theory. As it can be seen, rather good agreement between theory and experiment was obtained in all case, thus, this type of modeling might be useful to describe the observed release kinetics.

4. Mechanistic theories

Much more powerful than empirical and semi-empirical mathematical models are mechanistic theories. They can generally be used to get deeper insight into the underlying drug release mechanisms and potentially present a highly useful tool allowing to speed up the development of new products (via *in silico* simulations of the impact of formulation and processing parameters on drug release) (Siepmann et al., 2006; Siepmann and Siepmann, 2008).

A first example is shown in Fig. 5: the symbols represent the experimentally measured release of sodium salicylate from spherical beads based on Gelucire 46/07 (melting point = 46 °C, hydrophilic-lipophilic balance-value = HLB-value = 7). The release medium was simulated gastric fluid, the beads were prepared via melting. Three different types of devices were studied: (1) 264 mg beads with a radius of 0.36 cm, exposed to 200 mL release medium, (2) 187 mg beads with a radius of 0.33 cm, exposed to 200 mL release medium, and (3) 92 mg beads with a radius of 0.268 cm, exposed to 100 mL release medium. The curves in Fig. 5 represent fittings of the following equation (Crank, 1975):

$$\frac{M_t}{M_\infty} = 1 - \frac{6}{\pi^2}\sum_{n=1}^{\infty}\frac{1}{n^2}\cdot\exp\left(-\frac{Dn^2\pi^2 t}{R^2}\right) \quad (2)$$

where M_t and M_∞ represent the cumulative absolute amounts of drug released at time t and infinity, respectively; n is a dummy variable, R the radius of the beads and D the apparent diffusion coefficient of the drug within the system. This equation has been derived from Fick's second law of diffusion, considering the following conditions:

(i) The beads do not significantly swell or erode during drug release.
(ii) The beads are spherical in shape.
(iii) The drug is initially homogeneously distributed within the spheres.
(iv) Perfect sink conditions are provided throughout the experiments.
(v) Mass transfer resistance due to liquid unstirred boundary layers at the surface of the spheres is negligible compared to mass transfer resistance due to diffusion within the systems.
(vi) Drug dissolution is rapid and complete upon exposure to the release medium.
(vii) Diffusion with time- and position-independent diffusion coefficients is the release rate limiting mass transfer step.

As it can be seen in Fig. 5 good agreement between the fittings of Eq. (2) and the experimentally measured sodium salicylate release kinetics was obtained in all cases. Thus, diffusion seems to be the rate-limiting mass transport step in these systems, with time- and position-independent diffusion coefficients. However, it has to be pointed that that based on the available experimental data, it is not possible to distinguish between "drug diffusion control" and "water diffusion control": Eq. (2) also describes the penetration kinetics of a fluid into a spherical dosage form with constant diffusion coefficient and constant device dimensions. In this case, M_t and M_∞, represent the absolute cumulative amounts of liquid (e.g., water)

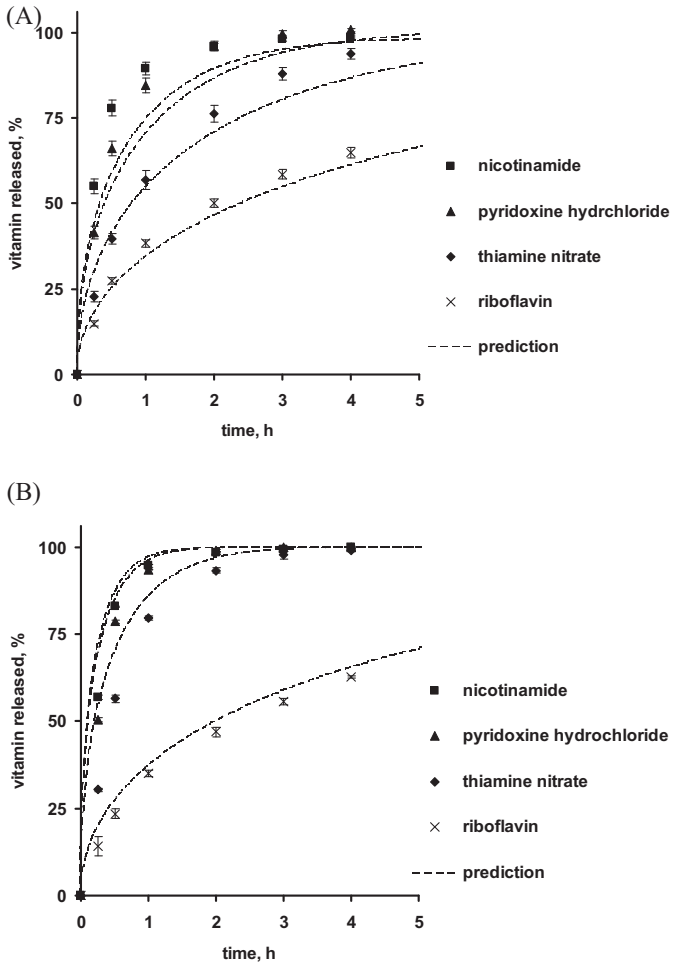

Fig. 6. Simultaneous controlled vitamin release from sucrose ester based granules prepared by: (A) melt granulation, or (B) compression & grinding (Sucrose Stearate S370; sucrose ester content: 80%, total vitamin content: 5%; release medium: phosphate buffer pH 6.8; the type of vitamin is indicated in the diagrams). The dashed curves show the theoretically predicted vitamin release kinetics (using Eq. (2)), the symbols the independent experimental verification.
Reprinted with permission from Seidenberger et al. (2011).

taken up by the system at time t, and infinite time, respectively; and D represents the apparent diffusion coefficient of the liquid (e.g., water). Assuming that *water*, and not *drug* diffusion is release rate-limiting, the same good agreement between experiment and theory (Eq. (2)) results (since the slowest process in a series of events is the determining one). In that case water penetration into the beads would be slow, whereas subsequent drug dissolution and diffusion would be fast. Consequently, the good agreement between theory and experiment observed in Fig. 5 might either be attributable to pure *drug* diffusion control, or to pure *water* diffusion control. Reports on the impact of the presence of surfactants in the release medium on the resulting drug release kinetics as discussed above (e.g., Fig. 3A versus Fig. 3B) might serve as indications for the "water diffusion control" hypothesis in such lipid dosage forms. In contrast, reports on significantly decreasing drug release rates from lipid implants with increasing molecular weight (and Stoke's radius) of the drug might serve as indications for the "drug diffusion control" hypothesis (Koennings et al., 2007b). It would be interesting to study this aspect in more detail in the future.

The above described "diffusion control theory" (Eq. (2) for spherical geometry) was also applied to quantify the simultaneous release of different vitamins (nicotinamide, pyridoxine hydrochloride, thiamine nitrate and riboflavin) from lipid granules based on sucrose esters (Seidenberger et al., 2011). The systems were prepared via melt granulation or compression & grinding. Importantly, in that study the mathematical model was also used to theoretically *predict* the resulting vitamin release kinetics from the systems, simulating the impact of the beads' size. Fig. 6 shows an example for such predictions. The apparent diffusion coefficient, D, of the vitamins in Sucrose stearate S370 (HLB value = 3) based granules were determined by fitting equation (2) to sets of release data obtained with the granule fraction 1.0–1.6 mm. Knowing these D-values, Eq. (2) was then used to theoretically predict nicotinamide, pyridoxine hydrochloride, thiamine nitrate and riboflavin release from smaller granules (fraction = 0.5–1 mm). These predictions are represented by the dashed curves in Fig. 6 (the granules in Fig. 6A were prepared via melt granulation, those in Fig. 6B via compression & grinding). Then, in a second step, the respective beads were prepared in reality and vitamin release was measured experimentally (symbols in Fig. 6). Clearly, good to rather good agreement was obtained in all cases, indicating the validity of this theory for this type of controlled drug delivery systems. Eq. (2) was also successfully used to theoretically predict the effects of the size of Gelucire 50/02 (melting point = 52 °C, HLB-value = 2) based beads containing theophylline (Siepmann et al., 2006). In that study, also an approximation of a slightly more complex theory, considering in addition limited drug solubility was applied (proposed by Koizumi and Panomsuk, 1995).

Deeper mechanistic insight into the control of drug release could also be obtained from lipid *implants*, based on the latter's physico-chemical characterization and mechanistic mathematical modeling (Guse et al., 2006a). Fig. 7A shows for example a macroscopic picture of a glyceryl tripalmitate based implant loaded with lysozyme, prepared by an emulsion-compression method: as it can be seen, the system is cylindrical in shape and provides smooth surfaces (note that also thinner cylinders can be prepared, allowing for injection via standard syringes and needles). A SEM picture of the surface of such an implant (prior to exposure to the release medium) is shown in Fig. 7B. Individual glyceryl tripalmitate plates can be clearly distinguished. These plates are crystalline and very poorly permeable for the drug and water. Thus, mass transport within this type of implants is likely to occur through the pores, which are located in-between the lipid plates. Guse et al. (2006a) assumed that diffusion is the dominant drug release mechanism and based their mathematical theory on Fick's second law for cylindrical geometry, considering axial and radial mass transport (Crank, 1975):

$$\frac{\partial c}{\partial t} = \frac{1}{r}\left\{\frac{\partial}{\partial r}\left(rD\cdot\frac{\partial c}{\partial r}\right) + \frac{\partial}{\partial \theta}\left(\frac{D}{r}\frac{\partial c}{\partial \theta}\right) + \frac{\partial}{\partial z}\left(rD\frac{\partial c}{\partial z}\right)\right\} \qquad (3)$$

where c is the concentration of the drug, t represents time; r, z denote the radial and axial coordinates and θ the angle perpendicular to the r–z-plane; D represents the apparent diffusion coefficient of the drug within the implant.

This partial differential equation was solved considering the given initial and boundary conditions, namely:

(i) The implants do not significantly swell or erode during drug release.
(ii) The implants are cylindrical in shape.
(iii) Diffusional mass transport occurs in radial and axial direction, with the same diffusivities.
(iv) The drug is initially homogeneously distributed within the implants.
(v) Perfect sink conditions are provided throughout the experiments.
(vi) Mass transfer resistance due to liquid unstirred boundary layers at the surface of the implants is negligible compared to mass transfer resistance due to diffusion within the systems.

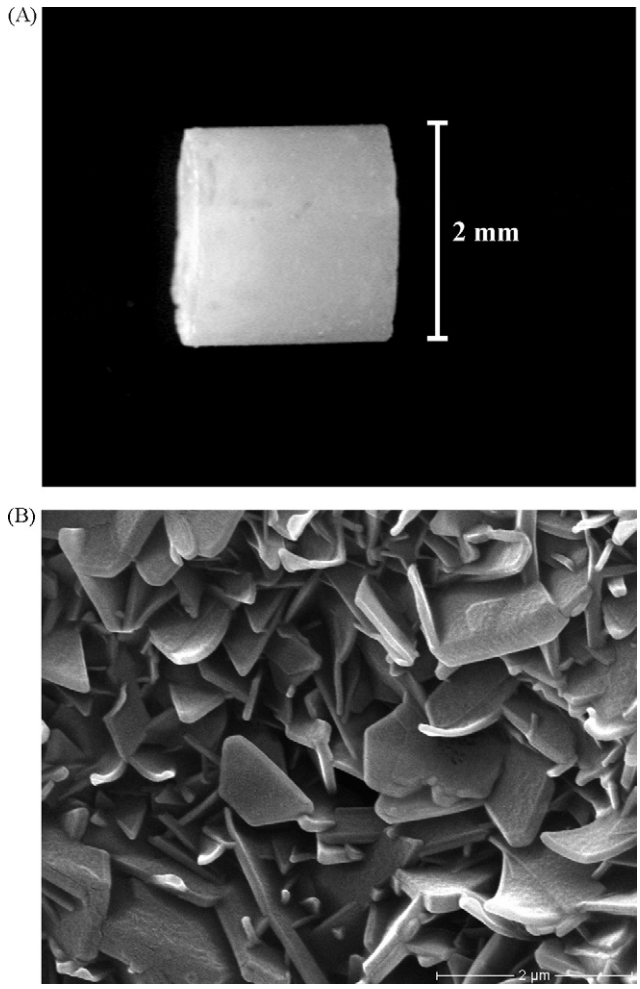

Fig. 7. Morphology of glyceryl tripalmitate based, lysozyme-loaded implants prepared by an emulsion-compression method: (a) optical microscopy picture of the entire implant, and (b) scanning electron microscopy picture of the surface of the implant (prior exposure to the release medium).
Reprinted with permission from Guse et al. (2006a).

(vii) Drug dissolution is rapid and complete upon exposure to the release medium.
(viii) Diffusion with time- and position-independent diffusion coefficients is the release rate limiting mass transfer step.

Using infinite series of exponential functions the following equation can be derived (Vergnaud, 1993):

$$\frac{M_t}{M_\infty} = 1 - \frac{32}{\pi^2}\sum_{n=1}^{\infty}\frac{1}{q_n^2}\exp\left(-\frac{q_n^2}{R_c^2}Dt\right)\cdot\sum_{p=0}^{\infty}\frac{1}{(2p+1)^2}\cdot\exp\left(-\frac{(2p+1)^2\pi^2}{H^2}Dt\right) \quad (4)$$

where M_t and M_∞ represent the absolute cumulative amounts of drug released at time t, and infinite time, respectively; q_n are the roots of the Bessel function of the first kind of zero order [$J_0(q_n) = 0$], and R and H denote the radius and height of the cylinder.

Fig. 8 shows examples for fittings of this theory (Eq. (4)) to sets of experimentally measured lysozyme release kinetics from implants based on glyceryl trilaurate, glyceryl trimyristate, glyceryl tristearate, or glyceryl tripalmitate (as indicated). The systems were prepared by an emulsion-compression method; the release medium was phosphate buffer pH 7.4. The symbols represent the experimentally measured protein release kinetics, the curves the fitted theory. As it can be seen, good agreement between theory and experiment was obtained in all cases, indicating that diffusional mass transport in axial and radial direction in these implants

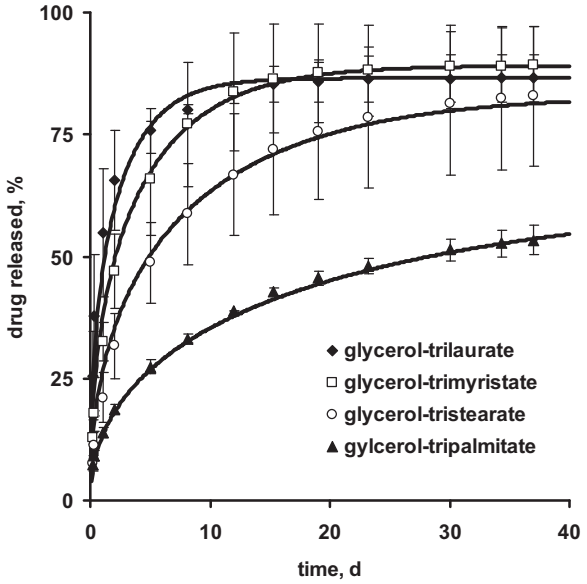

Fig. 8. Theory and experiment: effects of the type of matrix former (indicated in the diagram) on lysozyme release in phosphate buffer pH 7.4 from lipid implants prepared by an emulsion-compression method [symbols: experimental values, solid curves: fitted theory (Eq. (4))].
Reprinted with permission from Guse et al. (2006a).

is likely to be the dominant drug release mechanism. Again, note that either drug or water diffusion might be release rate controlling (in the latter case M_t and M_∞, represent the absolute cumulative amounts of water taken up at time t, and infinite time, respectively; and D denotes the apparent diffusion coefficient of water).

Kreye et al. (2011a) demonstrated the absence of significant swelling and erosion for various types of lipid implants, prepared by direct compression and loaded with propranolol hydrochloride or theophylline. Importantly, they could demonstrate that minor variations in the compression force and compression time period only moderately affected the resulting drug release patterns. Fig. 9

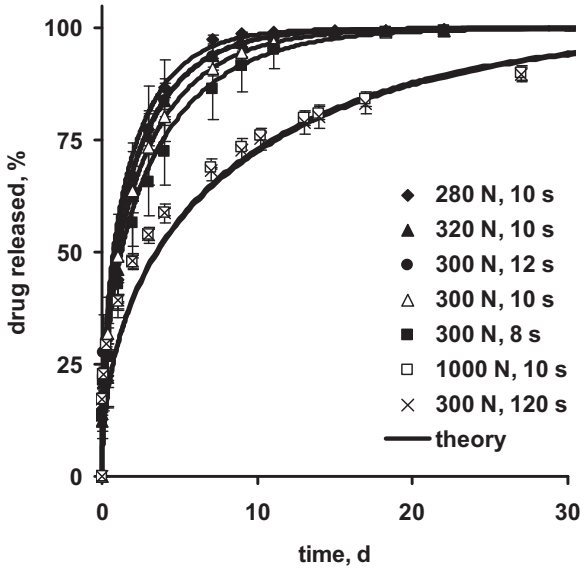

Fig. 9. Impact of the compression force and time (indicated in the diagram) on theophylline release from implants prepared by direct compression based on hydrogenated cottonseed oil in phosphate buffer pH 7.4 [symbols: experimental results; curves: fitted theory (Eq. (4))].
Reprinted with permission from Kreye et al. (2011a).

for example shows the release of theophylline from implants based on hydrogenated cottonseed oil in phosphate buffer pH 7.4. Varying the compression force from 280 to 320 N and the compression time from 8 to 12 s resulted in rather similar drug release profiles. However, when much higher compression forces (e.g., 1000 N), or much longer compression times (e.g., 120 s) were applied, the resulting theophylline release rate significantly decreased (Fig. 9). This is likely to be attributable to a denser packing of the lipid plates, resulting in narrower channels available for diffusion within the matrix. Interestingly, the dominant mass transport process remained to be diffusion in all cases: good agreement was observed, when fitting equation (4) to the experimentally determined drug release kinetics from these implants (curves and symbols in Fig. 9).

Later, Kreye et al. (2011) demonstrated that Eq. (4) can also be used to quantify drug release from lipid implants prepared by melting and casting (instead of compression). It has to be pointed out that special attention has to be paid to the physical state of the drug(s) and lipid(s) when using this manufacturing procedure: in case of polymorphisms, great care has to be taken that no changes occur during long term storage.

Despite these "positive examples", caution should be paid and significant deviations might be observed between a "pure diffusion control" theory (e.g., Eqs. (2) and (4) for spherical and cylindrical geometry) and experimentally measured drug release kinetics from lipid dosage forms. Fig. 10 shows some examples: propranolol hydrochloride release is illustrated from implants based on lipid blends: Precirol ATO 5 (glyceryl palmitostearate):Dynasan 120 (hardened soybean oil). The blend ratio is indicated in the diagrams, the release medium was phosphate buffer pH 7.4. In Fig. 10A drug release from the more rapidly releasing implants is shown, in Fig. 10B propranolol hydrochloride release from more slowly releasing systems. The symbols represent the experimental results, the curves the fitted theory (Eq. (4)). As it can be seen, only in two out of eleven cases, good agreement between theory and experiment was observed, in all other cases significant and systematic deviations resulted (solid curves indicate good agreement, dotted curves indicate poor agreement in Fig. 10). The poor agreement between the fitted theory (Eq. (4)) and the experimental results in the case of "pure" Dynasan 120 (hardened soybean oil) based implants (stars in Fig. 10B) can probably be attributed to the very limited amounts of water penetrating into these systems (Fig. 11). Thus, not all of the drug is dissolved and available for diffusion. Eq. (4) does not take such "limited drug solubility effects" into account. The poor agreement in the case of Precirol ATO 5 (glyceryl palmitostearate) contents >15% (Fig. 10A) can probably be explained by significant erosion of this compound during drug release. Fig. 11 also clearly shows that those implants took up more and more water with increasing Precirol ATO 5 content, with some exceptionally high values observed around 10–15% Precirol ATO 5. DSC studies and the analysis of the implants' mechanical properties confirmed particular system properties around this blend range, which can probably be attributed to limited mutual lipid solubility, resulting in phase separation in these implants.

As mentioned above, the physical state of the lipid(s) in the dosage forms needs to be controlled, especially if the systems are prepared via a melting step. To assure the presence of a desired, stable modification, a thermal after treatment (so-called "tempering" or "curing" step) might be helpful. For example, Kreye et al. (2011c) studied the impact of the tempering time (tempering temperature: 50 °C) on propranolol hydrochloride release from Sterotex NF (hydrogenated cottonseed oil) based implants prepared by melting & casting. Interestingly, the resulting drug release rate first increased with increasing tempering time, and then decreased again. Furthermore, propranolol hydrochloride release was mainly "diffusion-controlled" in the case of 7, 14 and 21 d tempering, but not in the case of 1 and 28 d tempering. This study is a good example for the fact that unexpected release behavior might be observed from lipid dosage forms, due to the complexity of the system. In this case it could be shown by thermal analysis that not polymorph transformations, but changes in the implants' microstructure were responsible for the altered drug release profiles (especially changes in the geometry and size of the channels located between the lipid particles). These modifications can alter the underlying drug release mechanisms (e.g., limited drug solubility effects might become more important, due to reduced amounts of water penetrating into the system).

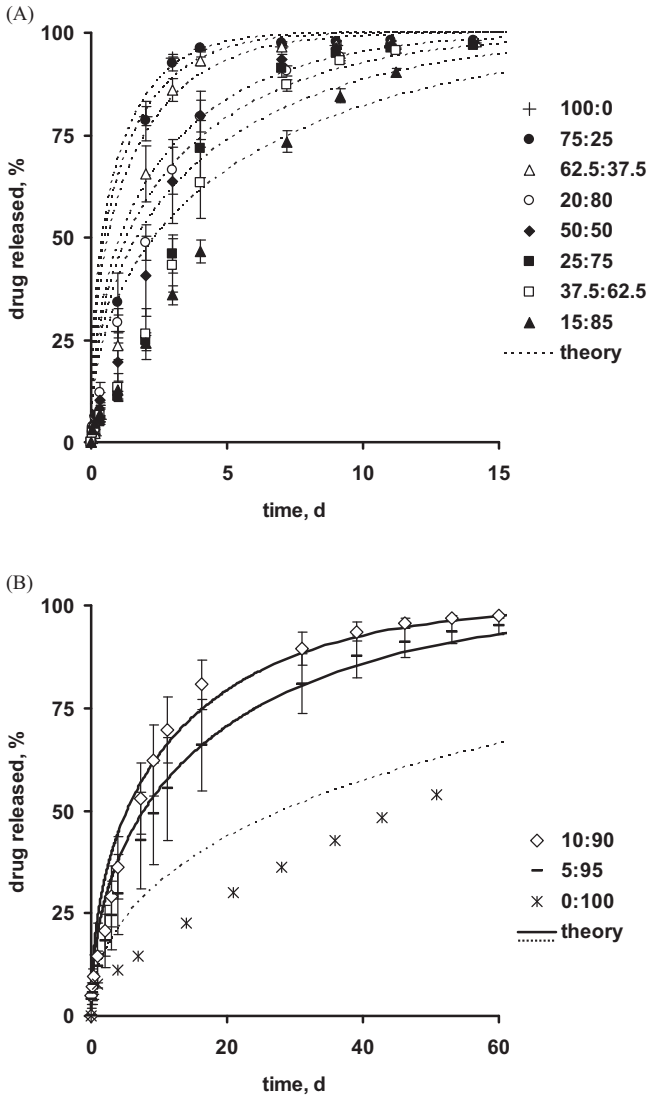

Fig. 10. Theory and experiment: propranolol hydrochloride release from Precirol ATO 5 (glyceryl palmitostearate):Dynasan 120 (hardened soybean oil) based implants (the blend ratio is indicated in the diagrams) into phosphate buffer pH 7.4: (A) more rapidly releasing implants, (B) more slowly releasing implants [symbols: experimental results; curves: fitted theory (Eq. (4)) (solid curves: good agreement; dotted curves: poor agreement)]. The implants were prepared via melting and casting.
Reprinted with permission from Kreye et al. (2011b).

If other excipients than the lipid matrix former are present in the dosage form, they should also be considered in the mathematical theory. For example, "pore formers", such as poly(ethylene glycol) (PEG) and protectants (e.g., hydroxypropyl-β-cyclodextrin = HP-β-CD) used during freeze drying of proteins might be added (Herrmann et al., 2007a). Upon contact with aqueous media such water-soluble excipients potentially leach out of the dosage form,

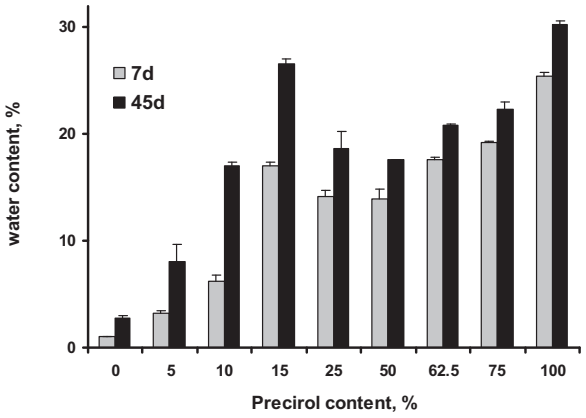

Fig. 11. Effects of the Precirol ATO 5 content in Precirol ATO 5 (glyceryl palmitostearate):Dynasan 120 (hardened soybean oil) based implants (prepared via melting and casting), loaded with 10% propranolol hydrochloride on the water content of the systems after 7 and 45 d exposure to phosphate buffer pH 7.4 (gray and black bars).
Reprinted with permission from Kreye et al. (2011b).

creating additional channels for water and drug diffusion. The symbols in Fig. 12A show for example the experimentally determined release kinetics of PEG out of glyceryl tristearate based implants prepared by compression into phosphate buffer pH 7.4. The PEG content in the implants was varied from 5 to 20%, as indicated. The systems contained 10% IFN-α/HP-β-CD. As it can be seen, the PEG leaching rate into the bulk fluid increased with increasing content of this "pore former", which can be attributed to the increasing size and number of channels available for water and PEG diffusion. Obviously, this phenomenon can be expected to have also a significant impact on drug release from these dosage forms. Thus, it is important to be able to quantitatively describe this process. The curves in Fig. 12A show fittings of Eq. (4) (with M_t and M_∞ representing the absolute cumulative amounts of PEG released at time t, and infinite time, respectively; and D denoting the apparent diffusion coefficient of PEG) to the experimentally measured leaching kinetics of this "pore former" (symbols). Clearly, good agreement between theory and experiment was observed in all cases, indicating that PEG diffusion is rate controlling. Fig. 12B illustrates the significant increase in the apparent PEG diffusion coefficient with increasing initial PEG content of the implants. Interestingly, the following quantitative relationship could be established:

$$D\ [10^{-8}\,\mathrm{cm^2/s}] = 0.7205 \cdot e^{0.1011 \cdot \text{initial PEG content [\%]}} \quad (5)$$

where D is the apparent diffusion coefficient of PEG. The fact that HP-β-CD leached out much more slowly from these implants than PEG can serve as an indication that indeed the diffusion of these two excipients is rate-limiting, and not the diffusion of water (otherwise, the leaching kinetics of PEG and HP-β-CD should be similar).

A further example for the fact that modeling drug release from lipid dosage forms can lead to a better understanding of the underlying mass transport mechanisms is illustrated in Fig. 13. The symbols represent the experimentally measured release of IFN-α from implants based on glyceryl tristearate prepared by compression into phosphate buffer pH 7.4. The systems initially contained 10% IFN-α/HP-β-CD and 10% PEG. The curve shows the best fitting of Eq. (4) ("pure diffusion control theory") to this set of data. Clearly, significant and systematic deviations occurred: protein release was overestimated at early time points and underestimated at late time points. Thus, not all of the phenomena, which significantly contribute to the control of drug release are adequately considered in the model. One of the reasons might be the negligence of the leaching of PEG and HP-β-CD into the release medium (which are not considered in Eq. (4)) when describing drug release: both processes

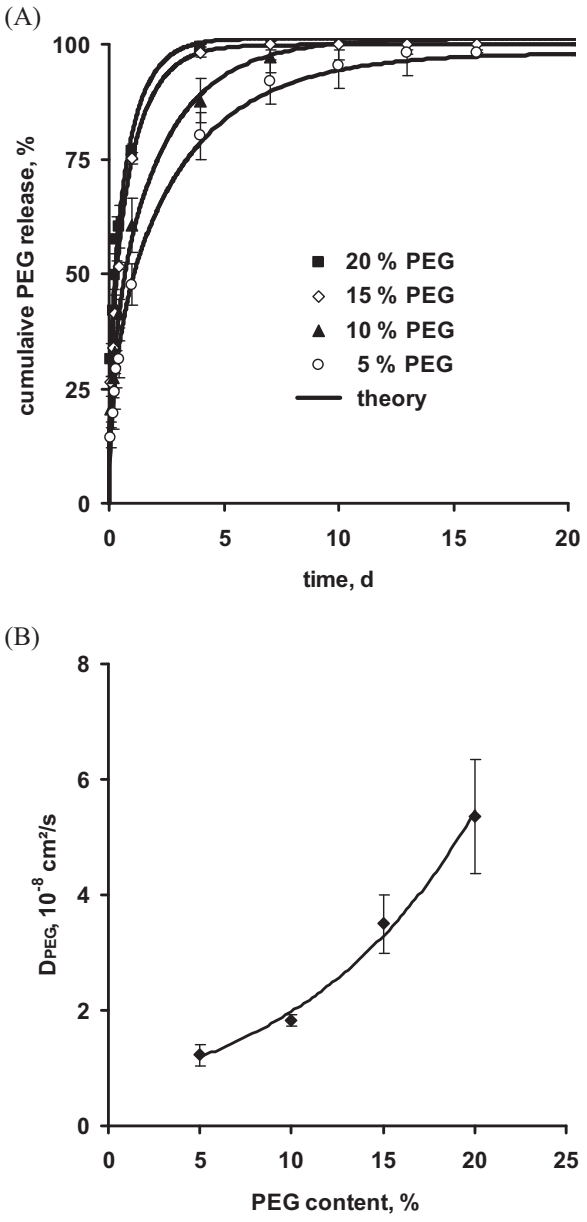

Fig. 12. Effects of PEG addition to glyceryl tristearate based implants prepared by compression on: (A) PEG release out of the systems into phosphate buffer pH 7.4: experiments (symbols) and theory (curves, Eq. (4)), (B) the apparent diffusion coefficient of PEG in the implants [determined by the fittings shown in (A)]. The devices were loaded with 10% IFN-α/HP-β-CD.
Reprinted with permission from Herrmann et al. (2007a).

can be expected to lead to increasing apparent diffusion coefficients of the protein with time. In addition, the solubility of IFN-α strongly depends on the concentration of co-dissolved PEG: as it can be seen in Fig. 14, the aqueous solubility of this protein drastically decreases with increasing PEG content (note that only values >4% PEG correspond to IFN-α solubility in this diagram). Thus, it can be expected that in the narrow channels located between the lipid particles high PEG concentrations might lead to significant drops in the aqueous solubility of the protein. Importantly, only *dissolved* IFN-α is able to diffuse. Also such limited solubility effects are not considered in Eq. (4).

In order to better understand these more complex types of lipid implants, a more comprehensive mathematical theory has been proposed (Siepmann et al., 2008). The model considers that:

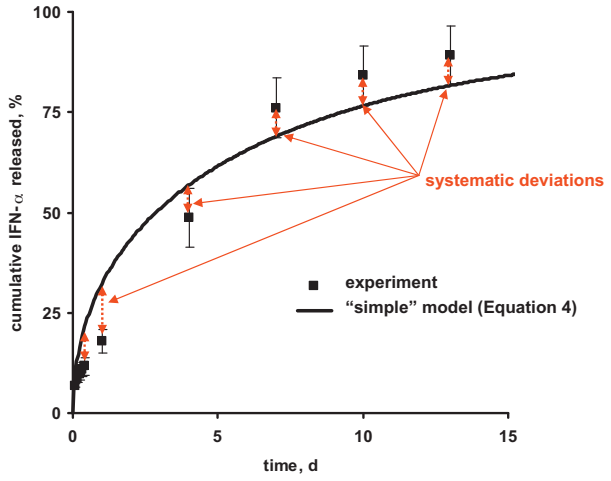

Fig. 13. Experiment (symbols) and "simple" theory (curve – Eq. (4)): IFN-α release into phosphate buffer pH 7.4 from glyceryl tristearate based implants prepared by compression, initially containing 10% IFN-α/HP-β-CD and 10% PEG.
Adapted from Herrmann et al. (2007b).

(i) The lipid implants are cylindrical in shape.
(ii) IFN-α, PEG, and HP-β-CD are homogeneously distributed throughout the devices before exposure to the release medium (at $t = 0$).
(iii) The implants are slightly porous at $t = 0$ (as determined using a helium pycnometer).
(iv) Upon contact with the release medium, water diffuses into the implants and IFN-α, PEG, and HP-β-CD simultaneously diffuse out of the systems (due to concentration gradients).
(v) The porosity of the lipid matrices steadily increases due to IFN-α, PEG, and HP-β-CD leaching (as confirmed with a helium pycnometer).
(vi) The increase in matrix porosity is time- and position-dependent (first surface-near regions become more and more porous, later on also the core of the implants).

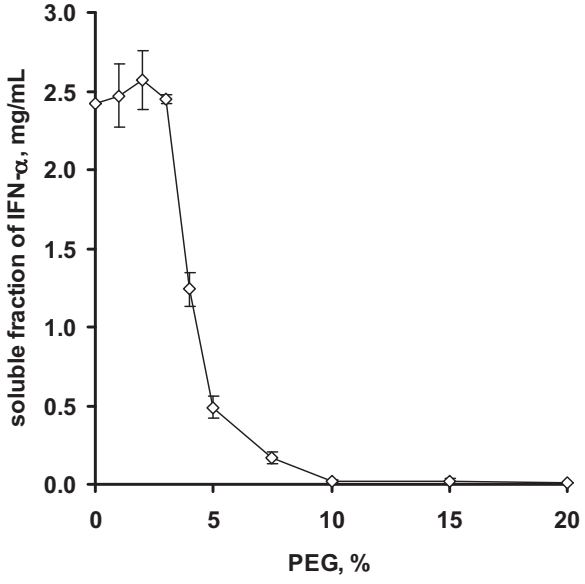

Fig. 14. Soluble fraction of IFN-α in phosphate buffer pH 7.4 at 37 °C as a function of the PEG content (average ± SD; $n = 3$) (values at ≥4% PEG correspond to the solubility of the protein under the given conditions).
Adapted from Herrmann et al. (2007b).

(vii) The diffusion coefficients of IFN-α, PEG, and HP-β-CD within the implants are directly related to the matrix porosity and are, hence, also position- and time-dependent (the diffusing species become more and more mobile with increasing implant porosity).
(viii) Water penetration into the matrix is much faster than the subsequent IFN-α, PEG, and HP-β-CD diffusion.
(ix) Diffusion occurs through water-filled pores; crystalline lipid plates are impermeable for IFN-α, PEG, and HP-β-CD.
(x) The solubility of IFN-α in the water-filled matrix pores strongly depends on the PEG concentration in these channels (the solubility of the protein strongly decreases with increasing PEG concentration, as shown in Fig. 14). At each time point and at each position, the actual PEG concentration and matrix porosity are calculated and used to determine the actual IFN-α solubility.
(xi) Non-dissolved IFN-α is not available for diffusion.
(xii) Diffusional mass transport occurs in radial as well as axial direction within the cylinders.
(xiii) Swelling or dissolution of the matrices is negligible within the observation period (visual observation).
(xiv) Perfect sink conditions are maintained throughout the experiments.

The quantitative description of simultaneous IFN-α, PEG, and HP-β-CD diffusion was based on Fick's second law considering the cylindrical geometry of the implants and taking into account axial and radial mass transfer with time- and position-dependent diffusion coefficients (thus, on Eq. (3), but considering 3 different diffusing species):

$$\frac{\partial c_k}{\partial t} = \frac{1}{r}\left\{\frac{\partial}{\partial r}\left(rD_k\frac{\partial c_k}{\partial r}\right) + \frac{\partial}{\partial \theta}\left(\frac{D_k}{r}\frac{\partial c_k}{\partial \theta}\right) + \frac{\partial}{\partial z}\left(rD_k\frac{\partial c_k}{\partial z}\right)\right\} \quad (6)$$

Here, c_k and D_k are the concentration and diffusion coefficient of the diffusing species ($k = 1$: drug; $k = 2$: PEG; $k = 3$: HP-β-CD), respectively; t represents time; and r, z and θ denote the radial, axial and angular coordinate, respectively. Fig. 15A shows a schematic presentation of such an implant for mathematical analysis. As there is no concentration gradient of any of the three components with respect to θ (Fig. 15B), this equation can be transformed into:

$$\frac{\partial c_k}{\partial t} = \frac{\partial}{\partial r}\left(D_k\frac{\partial c_k}{\partial r}\right) + \frac{D_k}{r}\frac{\partial c_k}{\partial r} + \frac{\partial}{\partial z}\left(D_k\frac{\partial c_k}{\partial z}\right) \quad (7)$$

To minimize computation time, the symmetry plane at $z = 0$ (Fig. 15A) can be taken into account. Consequently, it is sufficient to describe the changes in the IFN-α, PEG, and HP-β-CD concentrations within the 2-dimensional rectangle highlighted in Fig. 15B to be able to calculate the mass transport phenomena in the entire implant: upon rotation around the z-axis the upper half of the cylinder is described, and due to the symmetry at the $z = 0$ plane, the whole system can be considered. The initial conditions used to solve this set of partial differential equations were based on the fact that all three diffusing components are uniformly distributed throughout the implants before exposure to the release medium (at $t = 0$). As perfect sink conditions are provided for all diffusing species throughout the experiments, the IFN-α, PEG, and HP-β-CD concentrations at the surface of the implant can considered to be equal to zero upon exposure to the release medium. Importantly, due to the symmetries at $z = 0$ and $r = 0$ (Fig. 15A), there are no concentration gradients at $z = 0$ for $0 \le r \le R$ and at $r = 0$ for $0 \le z \le Z$ for any of the diffusing components. Furthermore, the limited aqueous solubility of IFN-α in the presence of dissolved PEG (Fig. 14) is taken into account in this more comprehensive mathematical model. In addition, the increase in IFN-α, PEG, and HP-β-CD mobility within

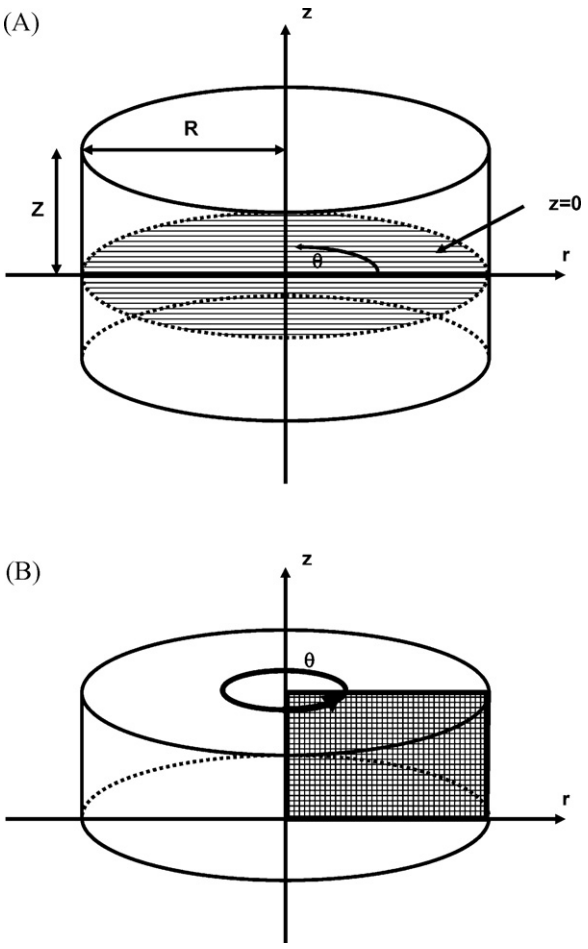

Fig. 15. Schematic presentation of a cylindrical lipid implant for mathematical analysis: (A) symmetry plane at $z = 0$, and (B) rotational symmetry with respect to the angle θ.
Reprinted with permission from Siepmann et al. (2008).

the lipid implants due to drug and excipient leaching is considered based on the following relationship:

$$D_k(r, z, t) = \frac{D_{k\ crit} \cdot \varepsilon(r, z, t)}{100} \quad (8)$$

where $D_{k\,crit}$ represents a critical diffusion coefficient, being characteristic for the diffusing species, and ε denotes the implant porosity in percent. Thus, the consequences of the dynamic changes in the implant structure during drug release on the conditions for the multi-component diffusion are quantitatively taken into account. As the matrix porosity increases upon IFN-α, PEG, and HP-β-CD leaching in a time- and position-dependent manner, there is no analytical solution for the above described set of partial differential equations and a numerical technique needs to be applied. For details the reader is referred to the literature (Crank, 1975; Smith, 1985; Vergnaud, 1991, 1993; Siepmann et al., 2008).

Importantly, this comprehensive mathematical model was able to quantitatively describe the experimentally measured IFN-α, PEG and HP-β-CD release kinetics from the investigated lipid implants and allowed gaining deeper insight into the underlying mass transport phenomena, for instance the time- and position-dependent excipient and drug concentrations as well as the solubility of the protein in the implants could be calculated. Fig. 16A and B shows two examples: the spatial solubility profiles of IFN-α within the implants are plotted after 1 and 3 d exposure to the release medium. Clearly, there are steep solubility gradients in both cases. Importantly, after 1 d exposure to the phosphate buffer, significant IFN-α

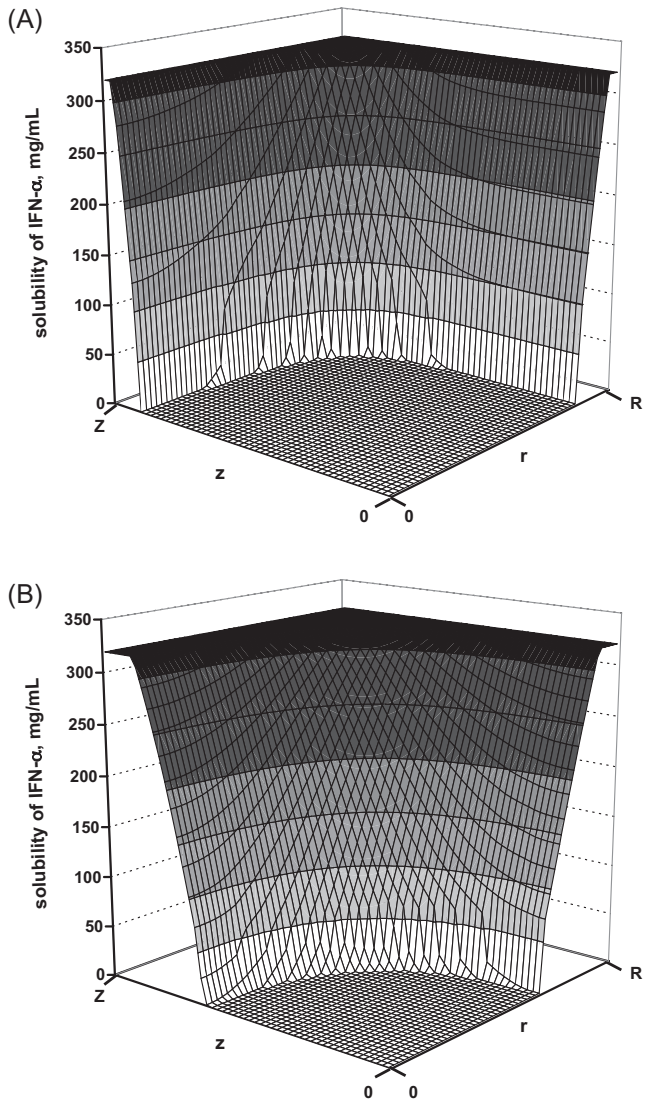

Fig. 16. Position- and time-dependent solubility of IFN-α within lipid implants prepared by compression, initially containing 10% IFN-α/HP-β-CD and 10% PEG, upon exposure to phosphate buffer pH 7.4: (A) solubility profile after 1 d exposure to phosphate buffer pH 7.4, (B) solubility profile after 3 d exposure to phosphate buffer pH 7.4.
Reprinted with permission from Siepmann et al. (2008).

solubility is very much limited to the outer parts of the implants. In contrast, after 3 d exposure more and more protein can be dissolved and become available for diffusion. Importantly, this more comprehensive mathematical is also able to quantitatively predict the impact of formulation parameters and device dimensions, thus, facilitating product optimization.

5. Conclusions and future outlook

Mathematical modeling of drug release from lipid dosage forms should be based on a thorough physico-chemical characterization of the systems. Various types of models have been proposed, which are more or less suitable for specific systems. Importantly, there is no overall theory, which is valid for all types of devices. Depending on the composition of the dosage forms more or less phenomena might be of importance, e.g. water and drug diffusion, limited drug solubility, and excipient leaching into the release medium. The great practical benefit of mechanistic mathematical theories is the possibility to quantitatively predict the impact of formulation

parameters and device dimensions on the resulting drug release kinetics. Since the targeted release periods might be long (e.g., several months), such *in silico* simulations can significantly speed up product development. For the future, it will be important to better characterize the *in vivo* release behavior of lipid dosage forms and to include the description of the fate of the drug in the living organism into the mathematical model, ideally also the pharmacodynamic effects of the treatment. This should for instance include diffusional and convective mass transport of the drug and excipients in the living body, drug metabolism, uptake into cells, enzymatic degradation of excipients and of the drug, mechanical stress exerted on the dosage form, drug binding to proteins and other molecules in the human organism, drug transport through membranes and interactions with target structures (such as receptors) as well as drug elimination.

Acknowledgements

The authors are grateful for the support of this work by the French National Research Agency "ANR" (BIOSTAB), the Nord-Pas de Calais Regional Council (PRIM) and the "INTERREG IVA 2 Mers Seas Zeeën Cross-border Cooperation Programme 2007-2013" (IDEA).

References

Allababidi, S., Shah, J.C., 1998. Kinetics and mechanism of release from glyceryl monostearate-based implants: evaluation of release in a gel simulating in vivo implantation. J. Pharm. Sci. 87, 738–744.
Bidah, D., Ouriemchi, E.M., Vergnaud, J.M., 1992. Diffusional process of drug delivery from a dosage form with a Gelucire matrix. Int. J. Pharm. 80, 145–149.
Crank, J., 1975. The Mathematics of Diffusion. Clarendon Press, Oxford.
Fan, L.T., Singh, S.K., 1989. Controlled Release: A Quantitative Treatment. Springer-Verlag, Berlin.
Guse, C., Koennings, S., Kreye, F., Siepmann, F., Goepferich, A., Siepmann, J., 2006a. Drug release from lipid-based implants: elucidation of the underlying mass transport mechanisms. Int. J. Pharm. 314, 137–144.
Guse, C., Koennings, S., Maschke, A., Hacker, M., Becker, C., Schreiner, S., Blunk, T., Spruss, T., Goepferich, A., 2006b. Biocompatibility and erosion behavior of implants made of triglycerides and blends with cholesterol and phospholipids. Int. J. Pharm. 314, 153–160.
Herrmann, S., Winter, G., Mohl, S., Siepmann, F., Siepmann, J., 2007a. Mechanisms controlling protein release from lipidic implants: effects of PEG addition. J. Control. Release 118, 161–168.
Herrmann, S., Mohl, S., Siepmann, F., Siepmann, J., Winter, G., 2007b. New insight into the role of polyethylene glycol acting as protein release modifier in lipidic implants. Pharm. Res. 24, 1527–1537.
Higuchi, T., 1961. Rate of release of medicaments from ointment bases containing drugs in suspension. J. Pharm. Sci. 50, 874–875.
Kaewvichit, S., Tucker, I.G., 1994. The release of macromolecules from fatty acid matrices: complete factorial study of factors affecting release. J. Pharm. Pharmacol. 46, 708–713.
Karasulu, E., Karasulu, H.Y., Ertan, G., Kirilmaz, L., Gueneri, T., 2003. Extended release lipophilic indomethacin microspheres: formulation factors and mathematical equations fitted drug release rates. Eur. J. Pharm. Sci. 19, 99–104.
Khan, M.Z.I., Tucker, I.G., Opdebeeck, J.P., 1991. Cholesterol and lecithin implants for sustained release of antigen: release and erosion in vitro, and antibody response in mice. Int. J. Pharm. 76, 161–170.
Khan, M.Z.I., Tucker, I.G., Opdebeeck, J.P., 1993. Evaluation of cholesterol-lecithin implants for sustained delivery of antigen: release in vivo and single-step immunisation of mice. Int. J. Pharm. 90, 255–262.
Koennings, S., Garcion, E., Faisant, N., Menei, P., Benoit, J.P., Goepferich, A., 2006. In vitro investigation of lipid implants as a controlled release system for interleukin-18. Int. J. Pharm. 314, 145–152.
Koennings, S., Berié, A., Tessmar, J., Blunk, T., Goepferich, A., 2007a. Influence of wettability and surface activity on release behavior of hydrophilic substances from lipid matrices. J. Control. Release 119, 173–181.
Koennings, S., Tessmar, J., Blunk, T., Goepferich, A., 2007b. Confocal microscopy for the elucidation of mass transport mechanisms involved in protein release from lipid-based matrices. Pharm. Res. 24, 1325–1335.
Koennings, S., Sapin, A., Blunk, T., Menei, P., Goepferich, A., 2007c. Towards controlled release of BDNF – manufacturing strategies for protein-loaded lipid implants and biocompatibility evaluation in the brain. J. Control. Release 119, 163–172.
Koizumi, T., Panomsuk, S.P., 1995. Release of medicaments from spherical matrices containing drug in suspension: theoretical aspects. Int. J. Pharm. 116, 45–49.
Kreye, F., Siepmann, F., Siepmann, J., 2008. Lipid implants as drug delivery systems. Expert Opin. Drug Deliv. 5, 291–307.
Kreye, F., Siepmann, F., Siepmann, J., 2011a. Drug release mechanisms of compressed lipid implants. Int. J. Pharm. 404, 27–35.
Kreye, F., Siepmann, F., Zimmer, A., Willart, J.F., Descamps, M., Siepmann, J., 2011b. Controlled release implants based on cast lipid blends. Eur. J. Pharm. Sci. 43, 78–83.
Kreye, F., Siepmann, F., Zimmer, A., Willart, J.F., Descamps, M., Siepmann, J., 2011c. Cast lipid implants for controlled drug delivery: importance of the tempering conditions. J. Pharm. Sci. 100, 3471–3481.
Kreye, F., Siepmann, F., Willart, J.F., Descamps, M., Siepmann, J., 2011. Drug release mechanisms of cast lipid implants. Eur. J. Pharm. Biopharm. 78, 394–400.
Mohl, S., Winter, G., 2004. Continuous release of rh-interferon α-2a from triglyceride matrices. J. Control. Release 97, 67–78.
Oezyazici, M., Goekçe, E.H., Ertan, G., 2006. Release and diffusional modeling of metronidazole lipid matrices. Eur. J. Pharm. Biopharm. 63, 331–339.
Opdebeeck, J.P., Tucker, I.G., 1993. A cholesterol implant used as a delivery system to immunize mice with bovine serum albumin. J. Control. Release 23, 271–279.
Peppas, N.A., 1985. Analysis of Fickian and non-Fickian drug release from polymers. Pharm. Acta Helv. 60, 110–111.
Schulze, S., Winter, G., 2009. Lipid extrudates as novel sustained release systems for pharmaceutical proteins. J. Control. Release 134, 177–185.
Schwab, M., Kessler, B., Wolf, E., Jordan, G., Mohl, S., Winter, G., 2008. Correlation of in vivo and in vitro release data for rh-INFα lipid implants. Eur. J. Pharm. Biopharm. 70, 690–694.
Schwab, M., Sax, G., Schulze, S., Winter, G., 2009. Studies on the lipase induced degradation of lipid based drug delivery systems. J. Control. Release 140, 27–33.
Seidenberger, T., Siepmann, J., Bley, H., Maeder, K., Siepmann, F., 2011. Simultaneous controlled vitamin release from multiparticulates: theory and experiment. Int. J. Pharm. 412, 68–76.
Siepmann, J., Goepferich, A., 2001. Mathematical modeling of bioerodible, polymeric drug delivery systems. Adv. Drug Deliv. Rev. 48, 229–247.
Siepmann, J., Peppas, N.A., 2001. Modeling of drug release from delivery systems based on hydroxypropyl methylcellulose (HPMC). Adv. Drug Deliv. Rev. 48, 139–157.
Siepmann, J., Siepmann, F., Florence, A.T., 2006. Local controlled drug delivery to the brain: Mathematical modeling of the underlying mass transport mechanisms. Int. J. Pharm. 314, 101–119.
Siepmann, J., Siepmann, F., 2008. Mathematical modeling of drug delivery. Int. J. Pharm. 364, 328–343.
Siepmann, F., Herrmann, S., Winter, G., Siepmann, J., 2008. A novel mathematical model quantifying drug release from lipid implants. J. Control. Release 128, 233–240.
Smith, G.D., 1985. Numerical Solution of Partial Differential Equations: Finite Difference Methods. Clarendon Press, Oxford.
Soo, P.L., Cho, J., Grant, J., Ho, E., Piquette-Miller, M., Allen, C., 2008. Drug release mechanism of paclitaxel from a chitosan–lipid implant system: effect of swelling, degradation and morphology. Eur. J. Pharm. Biopharm. 69, 149–157.
Vergnaud, J.M., 1991. Liquid Transport Processes in Polymeric Materials. Prentice-Hall, Englewood Cliffs.
Vergnaud, J.M., 1993. Controlled Drug Release of Oral Dosage Forms. Ellis Horwood, New York.
Wang, P.Y., 1989. Lipids as excipient in sustained release insulin implants. Int. J. Pharm. 54, 223–230.
Windbergs, M., Strachan, C.J., Kleinebudde, P., 2009. Understanding the solid-state behaviour of triglyceride solid lipid extrudates and its influence on dissolution. Eur. J. Pharm. Biopharm. 71, 80–87.
Yamagata, Y., Iga, K., Ogawa, Y., 2000. Novel sustained-release dosage forms of proteins using polyglycerol esters of fatty acids. J. Control. Release 63, 319–329.